

THIN-WALLED STEEL TUBULAR COLUMNS WITH UNIFORM AND GRADED THICKNESS UNDER CYCLIC LOADING

QUSAY AL-KASEASEBH and IRAJ H.P MAMAGHANI

Dept of Civil Engineering, University of North Dakota, Grand Forks, USA

Thin-walled steel tubular circular columns are widely used as cantilever bridge piers due to their geometric efficiency, aesthetic appearance, and high earthquake resistance. However, local buckling, global buckling, or interaction between both is usually the main reason of significant strength and ductility loss in these columns, which eventually leads to their collapse. This paper investigates the behavior of uniform circular (C) and graded-thickness circular (GC) thin-walled steel tubular columns under constant axial and cyclic lateral loading. The GC column with size and volume of material equivalent to the C column is introduced and analyzed under constant axial and cyclic lateral loading. The analysis carried out using a finite-element model (FEM), which considers both material and geometric nonlinearities. The accuracy of the employed FEM is validated based on the experimental results available in the literature. The results revealed that, significant improvements in strength, ductility, and post-buckling behavior of thin-walled steel columns obtained using the GC column.

Keywords: Circular section, Buckling, Ductility, Strength.

1 INTRODUCTION

Civil engineering structures are exposed to increased earthquake risks in severe seismic regions. Their integrity is always challenged due to extreme uncertainties of severe earthquakes (Miller 1998, Nakashima *et al.* 1998). Thin-walled steel tubular circular columns are widely used in modern buildings, offshore platforms, elevated storage tanks, and transmission towers (Ucak and Tsopelas 2006). In addition, they can be used in wind turbines and as cantilever bridge piers in seismic regions due to their geometric efficiency, aesthetic appearance, and high earthquake resistance (Ucak and Tsopelas 2014). Thin-walled steel tubular columns may be a superior to their counterparts of reinforced concrete due to their stiffness to cross-sectional area ratio, light-weight, and ductility, especially when limited construction space is preferable. However, local buckling, global buckling, or interaction between both is usually the main reason for a significant loss in strength and ductility in these members, which eventually leads to their failure under cyclic lateral loading (Mamaghani *et al.* 1996). Thin-walled steel tubular columns are susceptible to damage when subjected to strong earthquakes (i.e. the Kobe earthquake (1995), the Sichuan earthquake (2008), and the East Japan earthquake (2011)) and severe local buckling was reported in many studies (Bruneau 1998). As a result, several analytical and experimental studies were carried out to identify the factors, which might improve the strength and ductility of these columns under axial and cyclic lateral loading. Numerically, factors that affect the strength and ductility of circular tubular columns have been investigated (Gao *et al.* 1998b). Finite element

(FE) studies concluded that ductility of tubular circular columns is sensitive to the radius-to-thickness ratio parameter (R_t). Moreover, decreasing R_t and the column slenderness ratio parameter (λ) resulted in improvements on both strength and ductility of the columns (Gao *et al.* 1998a).

In this paper, a tested thin-walled steel tubular circular column (C) is numerically studied under constant axial and quasi-static cyclic lateral loading. The FE results are compared to the experimental results from literature to confirm the validity of the FE analysis. Moreover, a graded-thickness thin-walled steel tubular circular column (GC) is used with equivalent size and volume of material to C column in attempt to improve the strength, ductility, and post-buckling behavior. The main reason for the improved behavior of GC columns is their ability to eliminate severe local buckling near the base of the column where the buckling most likely occurs.

2 FINITE-ELEMENT ANALYSIS

There is no doubt that full-scale testing results in a better insight into understanding the structures' behaviors, however, physical experimentation is expensive and time consuming. For this purpose, FE analysis on the cyclic behavior of thin-walled steel tubular circular columns is carried out using ABAQUS Ver 6.14 (Hibbit *et al.* 2014). The FEM takes into account both material and geometric nonlinearities. The accuracy of FEM is validated based on the experimental results available in the literature (Nishikawa *et al.* 1998). The key parameters considered in the practical design of thin-walled steel tubular columns are radius-to-thickness ratio parameter (R_t), and column slenderness ratio parameter (λ) (Mamaghani and Packer 2002). R_t affects the local buckling behavior of thin-walled steel tubular circular columns, while λ controls the global buckling (Mamaghani 2008, Mamaghani and Packer 2002). R_t and λ parameters are determined as in Eq. (1) and Eq. (2):

$$R_t = \frac{D}{2t} \frac{\sigma_y}{E} \sqrt{3(1-\nu^2)} \quad (1)$$

$$\lambda = \frac{2h}{r} \frac{1}{\pi} \sqrt{\frac{\sigma_y}{E}} \quad (2)$$

Local buckling effect usually occurs near the base of C columns when they are subjected to constant axial load and cyclic lateral loading (Nishikawa *et al.* 1998). For this purpose, as shown in Figure 1, the upper part of the column is modeled using two-node beam element (B31), whereas four-node shell element (S4R), which considers accurately the local buckling, is used for the lower part of the column. All the elements are available in the ABAQUS library (Hibbit *et al.* 2014). The interface between the S4R and B31 elements is modeled using multi-point constraint (MPC). For computational efficiency, the bottom half of the lower part (D) is divided into 26 shell elements, while the remaining height (D) is only divided into 14 shell elements. The upper part of the column is divided into 14 beam elements. The above stated mesh divisions are determined by trial-and-error. It is found that such mesh density gives accurate results. The initial geometrical imperfection and residual stresses are not considered in the analysis, as their effects were not measured in the experiment (Hibbit *et al.* 2014). For thin-walled steel tubular columns, cyclic lateral load is more dominant than the axial load, which implies that the effect of the initial imperfections is negligible (Goto *et al.* 1998).

2.1 Cyclic Loading Program

The displacement-controlled unidirectional cyclic loading is illustrated in Figure 1d and adopted as a lateral loading program. The quasi-static cyclic loading is applied to the top of the column with the presence of the constant axial load (P) throughout the loading history. The cyclic displacement amplitude is increased as a multiple of the yield displacement (δ_y), which is calculated by Eq. (3):

$$\delta_y = \frac{H_y h^3}{3EI} \quad (3)$$

Where $H_y = (\sigma_y - P/A) Z/h =$ lateral yield load and A , h , EI , and $Z =$ cross-sectional area, the height, the bending stiffness, and the section modulus of the column, respectively (Goto *et al.* 2010). The yield displacements and lateral yield loads for the columns are listed in Table 1. All the analyzed columns are made of carbon steel SS400 (equivalent to ASTM A36 (2014)).

3 PROPOSED GC COLUMN

Conventional C columns experience premature buckling behavior in either local or global buckling form, near the base of the column, under constant axial and cyclic lateral loading. Under this buckling behavior, C columns are unable to fully utilize their strength and ductility capacities. To overcome these limitations, GC column is proposed as alternative for the counterpart C column. The column height and diameter are kept same for both C and GC columns. The GC column is divided into three segments of constant cross sections. The first and second segments have the same height that is equal to the diameter of the circular section from the base. The third segment has a height of $(h-2D)$. As shown in Figure 2, a thicker cross section ($t_1=1.25t$) is used along the first segment, and the original thickness ($t_2=t$) is kept for the second segment. Finally, the remaining material volume is distributed on the third segment with ($t_3=0.86t$). The above configurations of GC sections are chosen based on which achieved better behavior. Table 1 shows material and geometrical properties of C and GC columns. As can be seen, same material and geometrical properties (except the plate thickness) are used for both C and GC columns.

Table 1. Geometric and material properties of the C and GC columns.

Properties	C Column (Goto <i>et al.</i> 1998)	GC Column
Steel material	SS400	SS400
h (mm)	3403	3403
D (mm)	900	900
$t_1/t_2/t_3$ (mm)	9	11.25/ 9/ 7.75
λ	0.26	0.26
R_t	0.115	0.115
H_y (KN)	414.9	414.9
δ_y (mm)	10.6	10.6
$P/\sigma_y A_s$	0.124	0.124
σ_y (MPa)	298.6	298.6
σ_u (MPa)	495	495

4 COMPARISON OF NUMERICAL AND EXPERIMENTAL RESULTS

In this section, the numerical cyclic behavior results of the C columns are compared with the experiment results that were obtained by the Public Works Research Institute (PWRI) of Japan (Nishikawa *et al.* 1998).

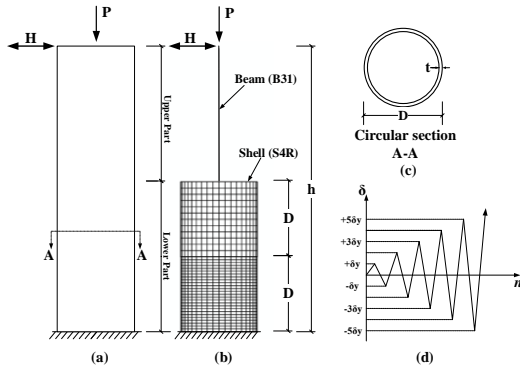


Figure 1. C Analytical model: (a) Bridge pier, (b) FE model, (c) Cross section, and (d) Loading program.

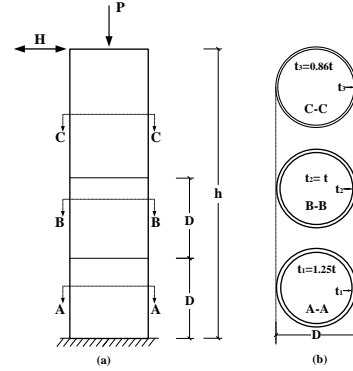


Figure 2. GC Analytical model: (a) Bridge pier, and (b) GC sections.

4.1 Hysteresis Curves of C and GC Columns

The analysis normalized lateral load vs. lateral displacement hysteresis curves, are shown in Figure 3. H_y and δ_y denote the lateral yield load and yield displacement, respectively. First, the FE analysis hysteresis loops are compared with experimental results available in the literature (Nishikawa *et al.* 1998). From Figure 3a, the comparison of hysteresis curves of C column, shows a reasonable agreement with the experimental results. This indicates that FE analysis, using kinematic hardening material behavior, gives a reasonable accuracy to describe the material behavior with regard of local buckling of thin-walled steel tubular columns. As shown in Figure 4, the deformed shape of C column (Figure 4b) at the end of the FE analysis is compared to the deformed shapes at the end of the experiment (Figure 4a) (Nishikawa *et al.* 1998). Based on this comparison, the deformed shape of C column is captured relatively well in the FE analysis. Using the same validated FEM, a comparison study has been performed between the behavior of the GC column and their counterpart C columns under the same axial and cyclic lateral loading. Figure 3b compares the hysteretic behavior of C and GC columns obtained from the FE analysis.

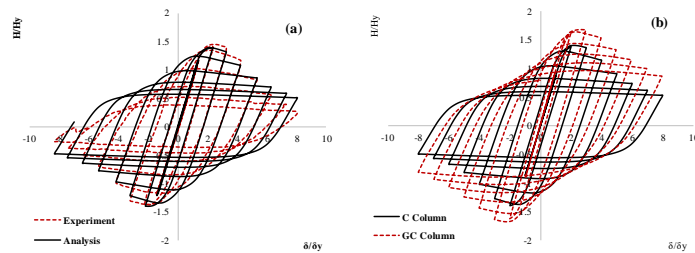


Figure 3. Horizontal load vs. horizontal displacement hysteretic curve.

In C column, the buckling initiates when the displacement is between $2\delta_y$ and $3\delta_y$. A strength drops of 17.6% of the ultimate column strength (observed at $\delta = +2.16\delta_y$) occurs at $\delta = +4\delta_y$. As the displacement increases, the column strength decreases at a rapid pattern to only 38% of its ultimate strength at $\delta = +8\delta_y$. On the other hand, GC column shows a maximum load capacity at

$\delta = +3\delta_y$. Only 8.4% strength drop of the ultimate strength took place at $\delta = +4\delta_y$, which gives an indication that local buckling started between $3\delta_y$ and $4\delta_y$. As the displacement amplitude is increased, more strength deterioration is observed. The residual strength of the GC column is 52% of its ultimate strength at $\delta = +8\delta_y$. It is worth mentioning that strength significantly drops at $\delta = -4\delta_y$, and $\delta = -8\delta_y$ for both columns. Generally, strength capacity improvement of 20% is obtained with the proposed GC column in comparison with the C column. Figure 4 shows the final deformed shapes of GC column compared to C column at $\delta = +8\delta_y$. For C column, buckling occurs near base as expected, while buckling shifted upward from the base in case of GC column.

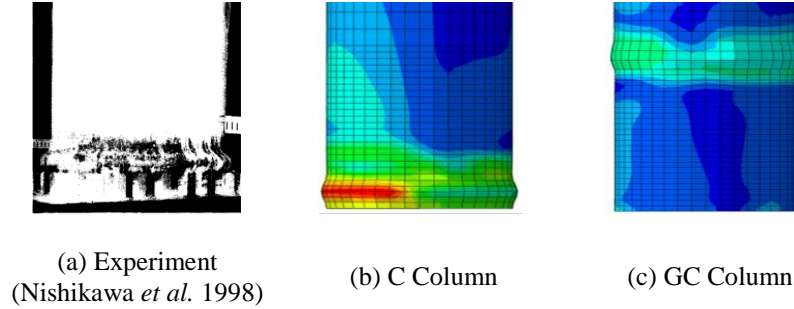


Figure 4. Deformation of columns.

5 ENERGY ABSORPTION CAPACITY

Ductility is the ability of a structure to resist large deformations. The dissipated energy is a measure of the cyclic behavior of the structures. Therefore, the energy absorption capacity of the C and GC columns has been studied. A normalized energy absorption (E) is defined in Eq. (4) (Mamaghani *et al.* 1996):

$$E = \frac{2}{H_y \delta_y} \sum_{i=1}^n E_i \quad (4)$$

In Eq. (4), E_i = energy absorption in the i -th half-cycle, n = number of half-cycles (one half-cycle is defined from any zero-lateral load to the subsequent zero-lateral load). Using the Eq. (4), Figure 5a compares the normalized cumulative energy absorption vs. n , obtained from the experiment and analysis of C column. The normalized energy absorption curves vs. n obtained from the analysis fit very close to the experimental results. For GC column, as shown in Figure 3b the strength of GC column decreases in a controlled rate from cycle to cycle compared to the C columns, which is expected to dissipate larger energy than the C column under cyclic lateral loading. Instead and by determining the area under lateral load vs. lateral displacement curves, Figure 5b shows that the dissipated energy of the GC column is larger than that of C column, which is expected to experience higher ductility in the case of proposed GC column.

6 CONCLUSIONS

In this paper, FE analysis has been carried out to evaluate the cyclic behavior of the C column. In addition, graded-thickness column (GC) equivalent to the C column is introduced in an attempt to improve the strength, ductility, and post-buckling behavior. First, the accuracy of the employed FEM was validated based on the experimental results available in the literature for the C column. The relatively good agreement between the FE analysis and experiment confirms the ability of the FEM to capture the structural behavior with regard of the local buckling of thin-walled steel

tubular circular columns. GC column shows a superior strength and ductility performance in comparison with the C column. An improvement of 20% in the ultimate strength was achieved using the GC column. Furthermore, improvements in the residual strength were observed in the case of GC column at the end of the analysis. The dissipated energy of the GC columns was higher which exhibited higher ductility. Buckling behavior of the C column was captured relatively well by the employed FEM. GC column delays the local buckling occurrence under cyclic lateral loading. Moreover, the buckled shape of the C column occurred near to the base as expected, while buckling shifted upward from the base in the GC column.

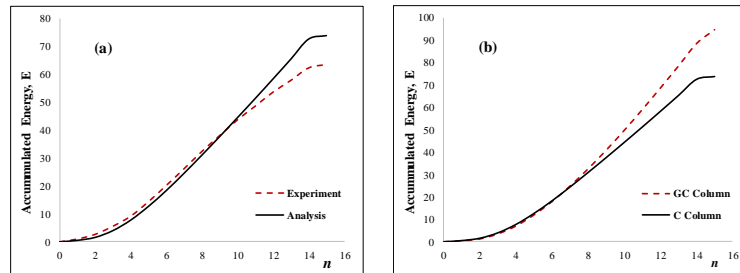


Figure 5. Energy absorption capacity.

References

- ASTM A36 / A36M - 14 Standard Specification for Carbon Structural Steel, *ASTM International, West Conshohocken, PA*, 12–14, 2014.
- Bruneau, M., Performance of Steel Bridges During the 1995 Hyogoken–Nanbu (Kobe, Japan) Earthquake—a North American Perspective, *Engineering Structures*, 20(12), 1063–1078, 1998.
- Gao, S., Usami, T., and Ge, H., Ductility Evaluation of Steel Bridge Piers with Pipe Sections, *Journal of Engineering Mechanics*, 124(3), 260, 1998a.
- Gao, S., Usami, T., and Ge, H., Ductility of Steel Short Cylinders in Compression and Bending. *Journal of Engineering Mechanics*, 124(2), 176–183, (1998b).
- Goto, Y., Kumar, G., and Kawanishi, N., Nonlinear Finite-Element Analysis for Hysteretic Behavior of Thin-Walled Circular Steel Columns with In-Filled Concrete, *Journal of Structural Engineering*, 136(11), 1413–1422, 2010.
- Goto, Wang, Q., and Obata, M., FEM Analysis for Hysteretic Behavior of Thin-Walled Columns, *Journal of Structural Engineering*, 124(11), 1290–1301, 1998.
- Hibbit, D., Karlsson, B., and Sorensen, P., *Abaqus 2014 Documentation*, Dassault, 2014.
- Mamaghani, I. H. P., Seismic Design and Ductility Evaluation of Thin-Walled Steel Bridge Piers of Box Sections, *Transportation Research Record: Journal of the Transportation Research Board*, 2050(1), 137–142, 2008.
- Mamaghani, I. H. P., and Packer, J. A., *Inelastic Behaviour of Partially Concrete-Filled Steel Hollow Sections*, 4th Structural Specialty Conference, 1–10, 2002.
- Mamaghani, I., Usami, T., and Mizuno, E., Cyclic Elastoplastic Large Displacement Behaviour of Steel Compression Members, *Journal of Structural Engineering*, 42, 135–145, 1996.
- Miller, D. K., Lessons Learned from the Northridge Earthquake, *Engineering Structures*, 20(4–6), 249–260, 1998.
- Nakashima, M., Inoue, K., and Tada, M., Classification of Damage to Steel Buildings Observed in the 1995 Hyogoken–Nanbu Earthquake, *Engineering Structures*, 20(6), 271–281, 1998.
- Nishikawa, K., Yamamoto, S., Natori, T., Terao, K., Yasunami, H., and Terada, M., Retrofitting for Seismic Upgrading of Steel Bridge Columns, *Engineering Structures*, 20(4–6), 540–551, 1998.
- Ucak, A., and Tsopelas, P., Cellular and Corrugated Cross-Sectioned Thin-Walled Steel Bridge-Piers/Columns, *Structural Engineering and Mechanics*, 24(3), 355–374, 2006.
- Ucak, A., and Tsopelas, P., Load Path Effects in Circular Steel Columns under Bidirectional Lateral Cyclic Loading, *Journal of Structural Engineering*, 141(2009), 1–11, 2014.